Effect of total percent polyacrylamide in capillary gel electrophoresis for DNA sequencing of short fragments

A phenomenological model

Heather R. Harke, Sue Bay, Jian Zhong Zhang, Marie Josée Rocheleau and Norman J. Dovichi

Department of Chemistry, University of Alberta, Edmonton, Alberta T6G 2G2 (Canada)

ABSTRACT

Polyacrylamide capillary gels were prepared with constant (5% C) cross-linker concentration and with total acrylamide concentration ranging from 2.5 to 6% T. At each acrylamide concentration, peak spacing was constant for DNA sequencing fragments ranging from 25 to 250 nucleotides in length. Peak spacing increased linearly with the total acrylamide concentration. The intercept of the retention time *vs.* fragment length plot was independent of %T. Ferguson plots were constructed for short DNA fragments; the polyacrylamide pore size falls in the 2.5 to 3.5 nm range for the gels studied. Theoretical plate count is independent of total acrylamide concentration; longitudinal diffusion, and not thermal gradients, limit the plate count. A phenomenological model is presented that predicts retention time, plate count, and resolution for sequencing fragments ranging in size from 25 to 250 bases and gels that range from 2.5 to 6% total acrylamide.

INTRODUCTION

DNA sequencing requires separation of labeled DNA fragments by denaturing gel electrophoresis. The separation rate of these fragments is proportional to the electric field strength; high electric fields lead to fast separations. However, Joule heating generates a temperature gradient that limits the maximum electric field strength. Because of the strong dependence of mobility on temperature, 2.3% per degree, thermal gradients can produce band-broadening and degradation of the separation at high electric field strengths in slab gels [1].

Conventional DNA sequencing slab gels are *ca.* 0.5 mm thick. Thinner gels, *ca.* 0.1 mm, generate fast and efficient separations [2–4]. Difficulties in automation, in maintaining a uniform gel thickness

across the slab, and in detection have retarded widespread applications of this technology. On the other hand, capillary gel electrophoresis offers highly uniform chambers and high sensitivity detection technology. Typical fused-silica capillaries of 50 μm I.D. produce outstanding thermal properties. Finally, the highly flexible nature of the capillaries simplifies automation.

Several groups have developed DNA sequencers based on capillary gel electrophoresis and laser-induced fluorescence detection [4–11]. In these systems, the capillaries are filled with denaturing polyacrylamide gels. The sequencing rate observed in these gels depends on the details of the gel composition. In this paper, we describe and model the sequencing rate, resolution, and separation efficiency in DNA sequencing by capillary gel electrophoresis.

Correspondence to: Dr. N. J. Dovichi, Department of Chemistry, University of Alberta, Edmonton, Alberta T6G 2G2, Canada.

EXPERIMENTAL

The two-spectral channel DNA sequencing capillary electrophoresis system has been described before [11]. The polyimide coated, fused-silica capillary (Polymicro, AZ, USA) is typically 35 cm long × 190 μm O.D. × 50 μm I.D. The gel formulae are described below. The injection end of the capillary is held in a Plexiglass box equipped with a safety interlock. The other end of the capillary is inserted into the flow chamber of a locally constructed sheath flow cuvette. Fluorescence is excited with a low-power argon ion laser (Uniphase, CA, USA) operating in the blue at 488 nm; fluorescence is collected at right angles with a microscope objective (Leitz/Wild, Calgary, Canada), imaged onto a pinhole, passed through a 525 nm center wavelength spectral filter (Omega, VT, USA), and detected with a photomultiplier tube (Hamamtsu, CA, USA). The current from the photomultiplier tube is dropped across a resistor, digitized, and recorded with a Macintosh IIsi computer.

The sample was prepared from a Genesis 2000 (DuPont, DE, USA) protocol using 3 μg M13mp18 single-stranded DNA, 15 ng – 21 17-mer M13 primer, and 2 μl Sequenase 2.0 (US Biochemicals, OH, USA) in a standard ddA terminating reaction mix. The sample was ethanol precipitated and washed and then resuspended in 4 μl of a mixture of formamide–0.5 M EDTA (49:1) at pH 8.0.

Gels are prepared in 5-ml aliquots from carefully degassed mixtures of acrylamide and N,N′-methylenebisacrylamide(Bis) 5%C, 2.5–6%T[a]; Bio-Rad, Toronto, Canada), 1X TBE, and 7 M urea (ICN, Montreal, Canada). Polymerization is initiated by addition of 2 μl of N,N,N′,N′-tetramethylethylenediamine (TEMED) and 20 μl of 10% ammonium persulfate. The solution is injected into the capillary by use of a syringe. To prevent deformation of the gel into the detection cuvette, the gel was covalently bound to the last *ca.* 5 cm of the capillary wall through use of γ-methacryloxypropyltrimethoxysilane [6]. Although polymerization appears complete in 30 min, the capillaries are typically stored overnight before use. With use of high purity reagents and careful degassing, more than 95% of

the gel-filled capillaries are bubble free and generated useful data. Two or three replicates were taken with each capillary.

The sample was injected at 150 V cm^{-1} for 30 s; after injection, the sample was replaced with a fresh vial of 1 × TBE. The electrophoresis continued at 150 V cm^{-1}. The sheath stream was 1 × TBE at a flow-rate of 0.10 ml/h. Time is measured from the application of the separation potential.

RESULTS AND DISCUSSION

Sequencing rate and retention time

Analysis was limited to 250 bases by the signal-to-noise ratio produced by this DNA sample. In all cases, a plot of retention time *vs.* fragment length (in bases) was linear ($r > 0.998$) for fragments ranging in size from the primer to at least 250 bases; that is,

$$\text{retention time} = T_0 + M \cdot \text{spacing} \quad (1)$$

where T_0 is intercept, spacing is the peak spacing in s/base, and M is the fragment length in bases. Fig. 1 presents typical data for a 4%T gel; for these data, T_0 is 21.0 min and the peak spacing is 8.0 s/base.

The peak spacing increased linearly with %T for all fragments (Fig. 2). The data are shown at the 95% confidence interval; the line is the result of an unweighted least-squares fit. Only two runs were made with the 3% gel, resulting in a large confidence interval. The slope of this line, 5.0 s/base per %T, implies that the peak spacing increases by 5 s for every 1% increase in total acrylamide concentration. The intercept, −9.9 s/base, should be related to the
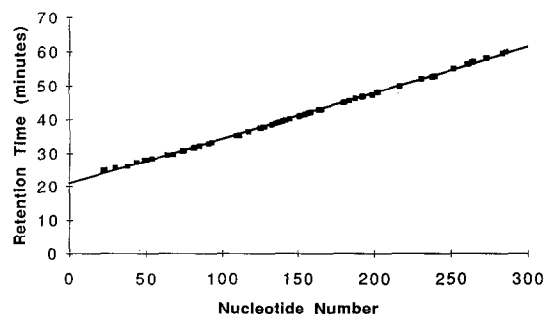

Fig. 1. Retention time as a function of fragment length for single-stranded DNA sequencing fragments separated in a 4%T, 5%C gel at an electric field strength of 150 V cm^{-1} in a 35 cm × 50 μm I.D. fused-silica capillary. The separation was at room temperature.

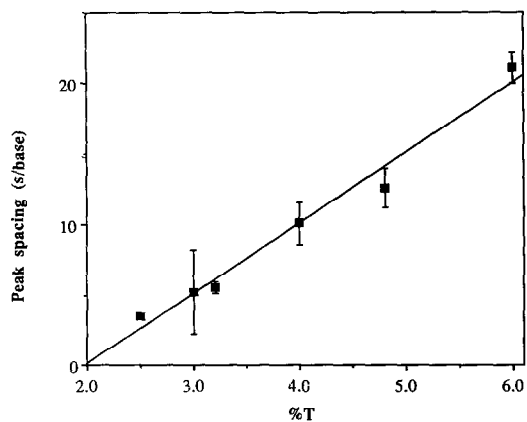[a] C = g Bis/%T; T = (g acrylamide + g Bis)/100 ml solution.

Fig. 2. Peak spacing of DNA fragments for denaturing polyacrylamide gels with constant 5%C, room temperature operation, an electric field strength of 150 V cm^{-1}, and a 35 cm × 50 μm I.D. capillary. The data are shown at the 95% confidence interval and the line is the unweighted least-squares fit with a linear function.

free solution mobility of the DNA fragments; presumably, the negative sign implies that longer fragments will have a higher mobility than shorter fragments. The data of Kambara et al. [12] data show a quadratic dependence of peak spacing on %T from 2 to 12%T; from 2 to 6%T, their data are similar to ours.

The inverse of peak spacing is sequencing rate (Fig. 3); the data in bases/h are shown at the 95% confidence interval. The sequencing rate observed
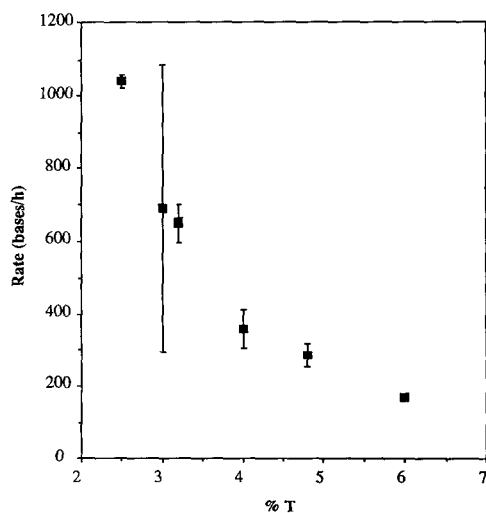

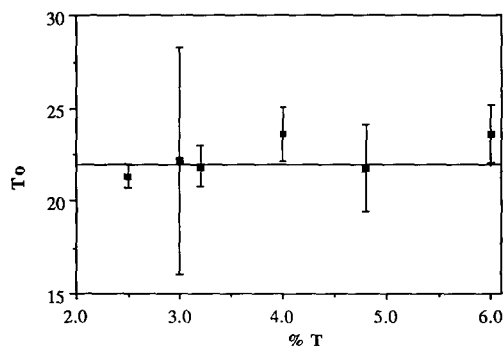Fig. 3. Sequencing rate for the data of Fig. 1. Data shown at the 95% confidence interval.

Fig. 4. Retention time for a vanishingly small DNA fragment as a function of total acrylamide concentration. Data shown at the 95% confidence interval.

for the 2.5% gel was 1,040 ± 10 bases/h, which is equal to the highest speed DNA sequencing rates reported in the literature for both capillary and slab gel electrophoresis [2,11].

Stegemann et al. [2] reported sequencing rate of 1000 bases/h for a slab gel separation at an electric field strength of 80 V cm^{-1}. Their data appears to have been generated at 50°C while our data were taken at room temperature, 20°C. The difference in electric field strength necessary to obtain this sequencing rate is due to the 2.3% °C^{-1} change in mobility with temperature [12].

T_0, the retention time for a vanishingly small DNA fragment, is independent of %T (Fig. 4); that is, the retention time of a hypothetical 0-base fragment does not change with %T. This independence of migration rate is not surprising because the 0-base fragment would experience no retardation by the gel; similar data are reported by Kambara et al. [12] for separations of single-strand DNA performed on slab gels at an electric field of 50 V cm^{-1}. The weighted average T_0 is 21.9 ± 0.2 min, shown as the horizontal line in the figure. Again, the data are shown at the 95% confidence interval. One datum was Q-tested at the 90% confidence level from the 6% gel data set.

Combining the results from Figs. 2 and 4, the retention time for a DNA fragment in a 5%C gel at 150 V cm^{-1} in a 35-cm long capillary at room temperature can be written as

retention time =

$$= 21.9 \text{ min} + M \cdot \%T \cdot 0.083 \text{ min/base/\%T} \quad (2)$$

for fragments ranging from 25 to 250 bases in length, gels ranging from 2.5 to 6%T, and room temperature operation. This formula was generated from over 35 electropherograms and represents over 80 h of instrument time.

Electrophoretic mobility

The relationship presented in eqn. 2 is quite robust in our laboratory. The equation is used to predict the electrophoretic mobility of a DNA sequencing fragment as a function of gel composition and nucleotide size.

$$\mu(M) = \frac{L/E}{\text{retention time}} \qquad (3)$$

where L is the length of the capillary and E is the electric field; the ratio $L/E = 0.233 \text{ cm}^2 \text{ V}^{-1}$ for our experimental conditions. The retention time relationship of eqn. 2 is substituted into eqn. 3 to predict the electrophoretic mobility of DNA fragments ranging in size from 25 to 250 bases and for gels ranging from 2.5 to 6%T.

$$\mu(M) = \frac{0.233 \text{ cm}^2 \text{ V}^{-1}}{1300 \text{ s} + M \cdot (-9.8 \text{ s/base} + 5.0 \text{ s/base} \cdot \%\text{T})} \qquad (4)$$

Eqn. 4 is a fundamental description of the electrophoretic behavior of nucleotides in 5%C polyacrylamide gels. This behavior must be described accurately for any successful theoretical description of DNA sequencing by gel electrophoresis.
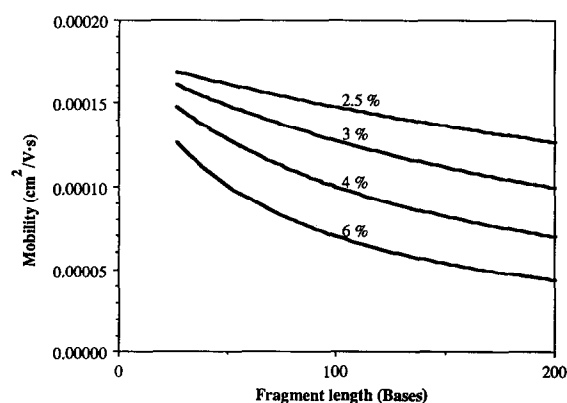

Fig. 5. Mobility of fluorescently labeled DNA fragments. Total percent acrylamide in the sequencing gel is noted above each curve.

Fig. 5 presents the predicted mobility for DNA fragments ranging from 25 to 200 bases in length and gels ranging from 2.5 to 6%T. The data extrapolate to a mobility of $1.8 \cdot 10^{-4} \text{ cm}^2 \text{ V}^{-1} \text{ s}^{-1}$ for a fragment of zero bases, independent of percentage acrylamide. The mobilities that we obtain are approximately a factor of two smaller than that reported by Holmes and Stellwagen [13] for double-strand DNA separated at an electric field strength of 3.3 V/cm and at room temperature. Our results are about 75% of the values reported by Kambara et al. [12] for separation of single-strand DNA in a slab gel at 48°C. The thermal coefficient of mobility, 2.3% °C^{-1}, exactly accounts for the observed difference between the data of Kambara et al. [12] and our data.

According to the Ogston model [13], mobility may be written as

$$\ln \mu(M) = \ln \mu(0) - K_R(M) \cdot \%\text{T} \qquad (5)$$

Using eqn. 4 to calculate mobility, Ferguson plots [13] were generated in the range of 2.5 to 6%T for fragments ranging in size from 25 to 100 bases. The Ogston model is fit to the data. The curves extrapolate to a common intercept, $\ln \mu(0) = -8.41 \pm 0.06$, corresponding to a mobility in free solution of $2.2 \pm 0.1 \cdot 10^{-4} \text{ cm}^2 \text{ V}^{-1} \text{ s}^{-1}$. This result is 25% higher than that estimated above from the peak spacing data and one half the value reported for double stranded DNA [13].

According to the Ogston theory, the retardation of fragments is related to the fractional volume of spaces in the matrix that are accessible to the analyte [13]. To find the %T that produces the same pore size as a particular DNA fragment, the gel composition is found that produces a mobility that is one-half that estimated for free solution. Taking the free solution mobility as $2.2 \cdot 10^{-4} \text{ cm}^2 \text{ V}^{-1} \text{ s}^{-1}$, the mobility of interest is $1.1 \cdot 10^{-4} \text{ cm}^2 \text{ V}^{-1} \text{ s}^{-1}$, or $\ln \mu = -9.12$. A 3.5%T gel is estimated to have a pore size of 3.5 nm, equal to the radius of a 100-mer single stranded fragment; a 4.1%T gel has a pore size of 3.2 nm, equal to the radius of a 75-mer, and a 5.2% T gel has a pore size of 2.8 nm, equal to the radius of a 50-mer. The DNA fragment size is estimated from the formula

$$\text{radius} = 0.755 \,(\text{bases})^{1/3} \qquad (6)$$
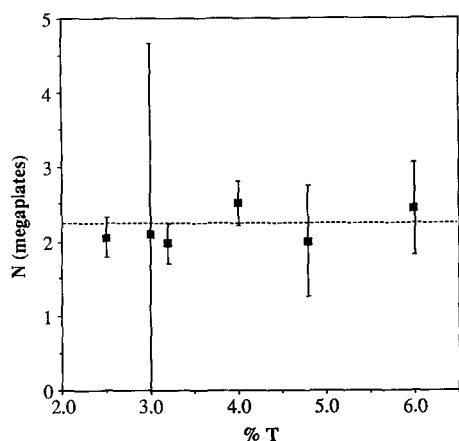
and is based on the geometric mean radius for

Fig. 6. Plate count for an 85-base DNA sequencing fragments as a function of total acrylamide concentration. Data are shown at the 95% confidence interval; the dotted line is the weighted average plate count.

double strand DNA [13]. A plot of log pore size *vs.* %T is linear ($r = 1.000$) over the range studied, with slope -0.56. These data are consistent with those observed for Ferguson plots produced on slab gels with double-stranded DNA [13].

Theoretical plates

The theoretical plate count for base 85 was independent of %T over the range studied, with a weighted average of $2.2 \pm 0.2 \cdot 10^6$ plates (Fig. 6). The data are shown at the 95% confidence interval and the dashed line is the weighted average plate count. Fragments 231 bases in length had separation efficiency, $N = 2.2 \pm 0.4 \cdot 10^6$ plates, that also was independent of %T. Plate counts were estimated from the second moment calculation. Slab gel data shows a similar independence of plate count on gel composition [12], although plate counts appear to increase slightly with fragment length.

Band broadening —injection, detection and thermal gradient

It is interesting to speculate on the origin of the constant plate count. The product of injection voltage and time was varied by several orders of magnitude to determine the effect of column overloading; no improvement in plate count was noted for the smallest sample loadings. Detection time constant and volume do not seem to be important;

the system response time would limit plate counts to *ca.* 100 million.

Thermal band broadening could contribute to plate count. Joule heating will produce a parabolic temperature profile in the capillary. For all the gels studied, the electric current was constant, $1.61 \pm 0.01 \ \mu A$, and independent of gel composition. The heat generated per unit volume in a capillary of radius r is

$$Q = \frac{EI}{r^2} = \frac{\lambda CV^2}{L^2} = \frac{150 \, V \, cm^{-1} \cdot 1.6 \cdot 10^{-6} \, A}{\pi (2.5 \cdot 10^{-3} \, cm)^2}$$
$$= 1.22 \cdot 10^1 \, W \, cm^{-3} \tag{7}$$

Note that the heat dissipated in the capillary scales with voltage squared, at constant molar conductance, λ, and ionic strength, C. Knox [14] has stated that the temperature difference between the axis of the capillary and the inner wall, θ, is given by

$$\theta = \frac{Qr^2}{4\kappa} = \frac{1.22 \times 10^1 \, W \, cm^{-3} \times (2.5 \times 10^{-3} \, cm)^2}{4 \times (4 \times 10^{-3} \, W/cm/K)}$$
$$= 0.005 \, K \tag{8}$$

where κ is the thermal conductivity of the solution, rather arbitrarily estimated as $4 \, mW \, cm^{-1} \, K^{-1}$ for the 7 M urea, 1 × TBE, polyacrylamide solution. The temperature difference across the capillary is very small for 50 μm I.D. capillaries at 200 V cm^{-1} electric fields.

The parabolic temperature profile is translated to a velocity profile by the relative thermal coefficient of mobility, $(d\mu/dT)/\mu = 0.023 \, K^{-1}$ [12] (where T = temperature). In our gels, the relative mobility of a fragment at the center of the capillary will be 0.00012 (0.012%) higher than the mobility of a fragment at the capillary wall. The maximum theoretical plate count in the presence of this thermally induced velocity profile is related to the diffusion coefficient of the DNA fragment; from the Stokes–Einstein formula, the diffusion coefficient of a molecule is given by [15]

$$D = \frac{kT}{6\pi\eta r_{molecular}} \tag{9}$$

where k is the Boltzmann constant. The data of Nishikawa and Kambara [1] suggest that the diffusion coefficient of a 100-mer fragment is about $1.0 \cdot 10^{-7} \, cm^2 \, s^{-1}$ at 50°C. Converting to 20°C, the

diffusion coefficient is expected to be about $9 \cdot 10^{-8}$ cm^2 s^{-1}. Substituting the diffusion coefficient, capillary length, fraction velocity difference, capillary radius, electrophoretic mobility, and electric field strength into Knox's equation

$$N_{thermal} = \frac{24 D_m L}{\left(\dfrac{d\mu/dT}{\mu}\theta\right)^2 r^2 \mu E} =$$

$$= \frac{24 \cdot 9 \cdot 10^{-8}\,\text{cm}^2\,\text{s}^{-1} \cdot 35\,\text{cm}}{\left[\begin{array}{c}(0.00012)^2(2.5 \cdot 10^{-3}\,\text{cm})^2 \cdot \\ \cdot (1.0 \cdot 10^{-4}\,\text{cm}^2\,\text{V}^{-1}\,\text{s}^{-1} \cdot 150\,\text{V}\,\text{cm}^{-1})\end{array}\right]}$$

$$= 5.6 \cdot 10^{10} \qquad (10)$$

yields $N_{thermal} = 56$ billion theoretical plates for an 86-mer fragment! Thermally induced band broadening does not appear to be significant in this capillary system.

$N_{thermal}$ scales inversely with the fifth power of electric field and thermally induced band-broadening is insignificant except at very high electric fields in capillaries. For example, an electric field strength of 800 V cm^{-1} will produce a temperature difference of 0.2°C across the 50 μm I.D. capillary, corresponding to $N_{thermal} = 5 \cdot 10^6$ plates. On the other hand, the thermal plate count scales inversely with the *sixth* power of radius. A 0.5-mm diameter capillary (with similar thermal characteristics as a 0.5-mm thick slab) will have a limiting plate count of 56 000 when operated at 150 V cm^{-1}. Thermal gradients dominate the performance of conventional slab gels at high electric fields.

Band broadening —longitudinal diffusion

Longitudinal diffusion appears to dominate band broadening in gel filled capillaries. Using the electrophoretic mobility of 85-mer fragments in 4% T gels, the plate count due to longitudinal diffusion is given by

$$N_{longitudinal} = \frac{\mu V}{2 D_m} =$$

$$= \frac{1.0 \cdot 10^{-4}\,\text{cm}^2\,\text{V}^{-1}\,\text{s}^{-1} \cdot 5250\,\text{V}}{2 \cdot 9 \cdot 10^{-8}\,\text{cm}^2\,\text{s}^{-1}} = 2.9 \cdot 10^6 \qquad (11)$$

which, given the assumptions in the estimation of diffusion coefficient, is in remarkable agreement with the data. The dependence of plate count on

fragment size can be estimated from the mobility formula of eqn. 4, the size dependence of DNA from eqn. 6, and the longitudinal diffusion equation above

$$N_{longitudinal} = \frac{\mu V}{2 D_m} =$$

$$= \frac{0.233 V}{\dfrac{1300\,\text{s} + M \cdot (-9.8\,\text{s/base} + 5.0\,\text{s/base} \cdot \%T)}{\dfrac{2kT}{6\pi\eta 0.755 M^{1/3}}}}$$

$$= \frac{A M^{1/3} V}{1300\,\text{s} + M \cdot (-9.8\,\text{s/base} + 5.0\,\text{s/base} \cdot \%T)} \qquad (12)$$

where A is a constant related to temperature and cross-linker concentration. For an 85-mer in a 4% T gel at a voltage of 5250 V, $A \approx 2.7 \cdot 10^5$ s V^{-1}. A plot of expected plate count *vs.* fragment length is shown in Fig. 7. Plate count maximizes for short fragments, *ca.* 85-mer, but varies by only 25% for fragments ranging in size from 25 to 250 bases. Within experimental error, plate count is independent of fragment length.

Plate count should increase linearly with applied potential. Potential can be increased either by increasing the electric field strength, for a constant length capillary, or by increasing the length of the capillary, at constant applied potential. The electric field strength cannot be increased without bounds. Polyacrylamide gels are unstable at electric field strengths greater than about 500 V cm^{-1} in our
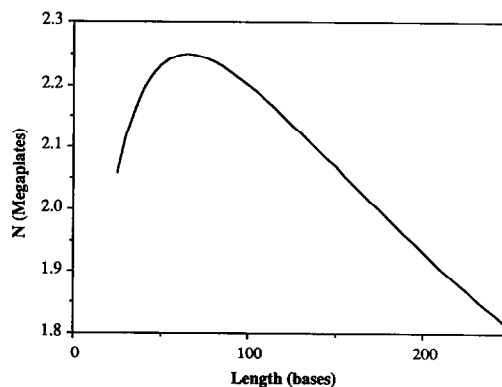

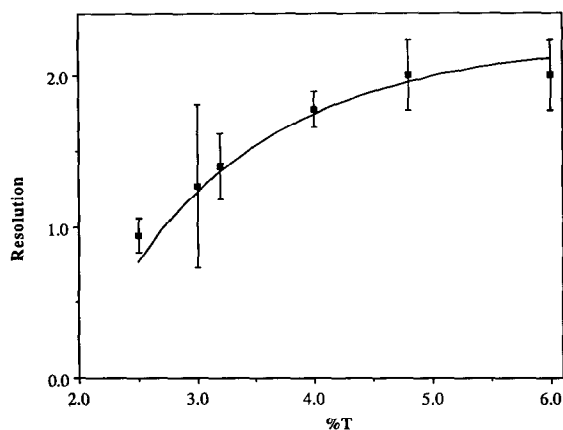Fig. 7. Predicted plate count in a 4% total acrylamide gel.

Fig. 8. Resolution of bases 85–86. Data are shown at the 95% confidence interval. The smooth curve is the prediction of eqn. 14; no parameters were adjusted.

laboratory. Large bubbles form in the capillary at high fields, destroying the separation. However, microbubbles may form at intermediate potentials, creating eddy diffusion and degrading the separation efficiency. It appears that longer capillaries are required to produce very high separation efficiency, albeit at the expense of longer analysis time.

Resolution

Resolution was determined graphically for peaks 85–86 at different %T. The data are shown at the
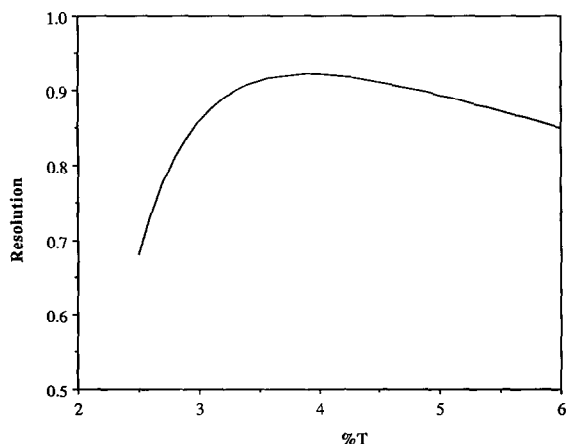

Fig. 9. Predicted resolution for adjacent DNA fragments as a function of total acrylamide concentration for fragments 250–251 bases in length.

95% confidence interval in Fig. 8. The range of resolution observed for the data, from 1 to 2, is quite similar to results from slab gel data [12]. Resolution degraded with increased length of sequencing fragments, for all %T studied; a similar phenomenon is present in the data of Kambara et al. [12] for fragments ranging in size from 100 to 400 bases.

Resolution of adjacent peaks is related to the theoretical plate count and the relative peak spacing [16,17]

$$\text{resolution} = \frac{\sqrt{N}}{4} \cdot \frac{\text{spacing}}{t_r} \qquad (13)$$

substituting expressions for plate count, peak spacing, and retention time, the resolution is predicted to be

$$\text{resolution} =$$

$$\frac{\sqrt{A M^{1/3}\,V} \cdot \frac{1}{4} \cdot (-9.84\,\text{s/base} + 4.99\,\text{s/base} \cdot \%T)}{[1310\,\text{s} + M \cdot (-9.84\,\text{s/base} + 4.99\,\text{s/base} \cdot \%T)]^{3/2}}$$

$$(14)$$

The smooth curve in Fig. 8 is a plot of predicted resolution for a fragment 82 bases in length and a potential of 5250 V. Recalling that there are no adjustable parameters in the theory, the agreement with the data is outstanding.

Resolution decreases as ca. $M^{-3/2}$ for larger fragments at constant gel composition. For any given length fragment, resolution is maximized for a particular gel composition. Fig. 9 presents a plot of resolution vs. % T for a fragment 250 bases in length. Under the conditions at which our gels are run, the optimum resolution for a 250-mer is produced with a 4%T gel. To analyze long DNA fragments, it is appropriate to use low %T gels.

CONCLUSIONS

We have presented a phenomenological model of DNA sequencing in polyacrylamide gels with 5% cross-linker concentration. The mobility model has three parameters: fragment length, %T, and the retention time of a vanishingly small DNA fragment. The plate count and resolution model contains one additional parameter, the diffusion coeffi-

cient of a DNA fragment of known size in a gel of known concentration.

This model is limited to 5%C polyacrylamide gels ranging from 2.5 to 6%T and operating at 150 V cm^{-1} at room temperature. Based on slab-gel data, eqn. 1 requires a quadratic term to describe sequencing data for gel compositions extending to 10%T. Because mobility increases by 2.3% per degree temperature rise, faster separations are expected at higher temperatures. Similarly, different cross-linker concentration or composition will lead to different sequencing rates.

The phenomenological model presented in this paper is limited to short fragments at an electric field strength of 150 V cm^{-1}. Our model is expected to fail for longer fragments and higher electric fields. Theory for double stranded DNA states that short fragments at low electric field exist in a random coil configuration [18]; the mobility of these fragments scale inversely with size. At higher electric fields, or for longer fragments, there is a transition to a stretched or linear configuration; these fragments migrate independently of size. Of course, it is not possible to obtain sequence information from fragments in the linear configuration. For double stranded DNA, the transition from random coil to stretched rod configuration scales as M/E^2 [18]. Extrapolation of our model to fragments longer than 250 bases or for electric fields higher than 150 V cm^{-1} is not warranted.

ACKNOWLEDGEMENTS

REFERENCES

1 T. Nishikawa and H. Kambara, *Electrophoresis*, 12 (1991) 623.
2 J. Stegemann, C. Schwager, H. Erfle, N. Hewitt, H. Voss, J. Zimmermann and W. Ansorge, *Nucleic Acids Res.*, 19 (1991) 675.
3 A. J. Kostichka, M. K. Marchbanks, R. L. Brumley, H. Drossman and L. M. Smith, *Bio/Technology*, 10 (1992) 78.
4 H. Swerdlow and R. Gesteland, *Nucleic Acids Res.*, 18 (1990) 1415.
5 H. Drossman, J. A. Luckey, A. J. Kostichka, J. D'Cunha and L. M. Smith, *Anal. Chem.*, 62 (1990) 900.
6 A. S. Cohen, D. R. Najarian and B. L. Karger, *J. Chromatogr.*, 516 (1990) 49.
7 H. Swerdlow, S. Wu, H. Harke and N. J. Dovichi, *J. Chromatogr.*, 516 (1990) 61.
8 J. A. Luckey, H. Drossman, A. J. Kostichka, D. A. Mead, J. D'Cunha, T. B. Norris and L. M. Smith, *Nucleic Acid Res.*, 18 (1990) 4417.
9 D. Y. Chen, H. P. Swerdlow, H. R. Harke, J. Z. Zhang and N. J. Dovichi, *J. Chromatogr.*, 557 (1991) 237.
10 A. E. Karger, J. M. Harris and R. F. Gesteland, *Nucleic Acids Res.*, 19 (1991) 4955.
11 H. Swerdlow, J. Z. Zhang, D. Y. Chen, H. R. Harke, R. Grey, S. Wu, N. J. Dovichi and C. Fuller, *Anal. Chem.*, 63 (1991) 2835.
12 H. Kambara, T. Nishikawa, Y. Katayama and T. Yamaguchi, *Bio/Technology*, 6 (1988) 816.
13 D. L. Holmes and N. C. Stellwagen, *Electrophoresis*, 12 (1991) 253.
14 J. H. Knox, *Chromatographia*, 26 (1989) 329.
15 R. A. Mosher, D. Dewey, W. Thormann, D. A. Saville, M. Bier, *Anal. Chem.*, 61 (1989) 362.
16 J. W. Jorgenson, K. D. Lukacs, *Anal. Chem.*, 53 (1981) 1298.
17 J. C. Giddings, *Sep. Sci.*, 4 (1969) 181.
18 J. Noolandi, *Can. J. Phys.*, 68 (1990) 1055.